CONCEPTS FOR A THEORETICAL AND EXPERIMENTAL STUDY OF LIFTING ROTOR RANDOM LOADS AND VIBRATIONS

(Development of Experimental Methods)

Phase V-C Report under Contract NAS2-4151

by

Kurt H. Hohenemser

and

S. T. Crews

Department of Mechanical and
Aerospace Engineering

Washington University
School of Engineering and Applied Science
St. Louis, Missouri

June, 1971

CONCEPTS FOR A THEORETICAL AND EXPERIMENTAL STUDY OF LIFTING ROTOR RANDOM LOADS AND VIBRATIONS

(Development of Experimental Methods)

Phase V-C Report under Contract NAS2-4151

by

Kurt H. Hohenemser

and

S. T. Crews

Department of Mechanical and
Aerospace Engineering

Washington University
School of Engineering and Applied Science
St. Louis, Missouri

June, 1971

CONCEPTS FOR A THEORETICAL AND EXPERIMENTAL STUDY OF LIFTING ROTOR RANDOM LOADS AND VIBRATIONS

(Development of Experimental Methods)

Phase V-C Report under Contract NAS2-4151

Prepared for the Ames Directorate, AMRDL,
at Ames Research Center, Moffett Field, California

by Kurt H. Hohenemser

Kurt H. Hohenemser

and S. T. Crews

S. T. Crews

Washington University
School of Engineering and Applied Science
St. Louis, Missouri

June, 1971

Scope of Contract NAS2-4151

Work under Contract NAS2-4151 started on February 1, 1967. Phase I Report of September 1967 develops analytical concepts for a random loads and vibrations analysis of lifting rotors. Phase II Report of August 1968 presents a perturbation solution method for random blade flapping. Phase III Report of June 1969 develops a more general method to include high rotor advance ratios and makes use of a specific atmospheric turbulence model. Phase IV Report of June 1970 extends the method to the computation of threshold crossing statistics for random blade flapping and introduces non-uniformity of the vertical turbulence velocity in the longitudinal direction. During FY 1971 the work was extended in three directions, resulting in 3 separate Phase V reports. Phase V-A Report covers the inclusion of blade torsional flexibility in the blade random gust response statistics. Phase V-B Report covers the analysis of lifting rotor gust alleviation methods and rotor dynamic stability. Phase V-C Report describes the efforts to develop experimental methods of substantiating the random loads and vibration analysis. The work summarized in Phase V-A Report was performed under Modification 5 to subject contract. The work summarized in Phase V-B and Phase V-C Reports was performed under Modification 6 to subject contract. A proposal has been submitted

for an extension of Contract NAS2-4151 through FY 1972 and FY 1973. The scope of the proposed extension is to remove some of the limitations of the present analytical model and at the same time simplify the method of analysis, and to conduct model tests to support the analysis.

CONCEPTS FOR A THEORETICAL AND EXPERIMENTAL STUDY OF LIFTING ROTOR RANDOM LOADS AND VIBRATIONS

Phase V-C
(Development of Experimental Methods)

by
Kurt H. Hohenemser
and
S. T. Crews

Washington University
St. Louis, Missouri

Abstract

This report describes the test equipment which has been built, and the calibration tests. The test equipment consists of a two-bladed rotor of 16 inches diameter where the blades are elastically hinged in flapping. The feathering shaft of the blades can be harmonically rotated with the help of a cam mechanism located inside the hollow rotor shaft. The frequency range measured in the rotating system can be adjusted between 0 and 80 cps, while the rotor speed can be adjusted between 0 and 40 cps. The purpose of the test equipment is to measure the flapping response of the blades to harmonic feathering excitation. Rotor advance ratios up to 1.6 are scheduled to be tested in the 2 x 2 ft section of the available wind tunnel. The test results are to be compared with the results of the linearized analysis which was used in the preceding random blade flapping studies.

CONCEPTS FOR A THEORETICAL AND EXPERIMENTAL STUDY OF LIFTING ROTOR RANDOM LOADS AND VIBRATIONS

Phase V-C

(Development of Experimental Methods)

Table of Contents

List of Figures

1. Introduction

The studies of blade random flapping responses to atmospheric turbulence presented in Phase I to Phase IV Reports under Contract NAS2-4151 and in References (1) to (3) made use of a linear flapping analysis including reversed flow effects given in Reference (4). Because of the numerous assumptions made in this analysis it was believed appropriate to check the validity range of the analysis against some test results. The analysis ignores stall effects, compressibility effects, non-steady aerodynamic effects, effects from blade flexibility, effects from flapping hinge off-set and assumes uniform inflow over the rotor disk. The analysis of Reference (4), because it includes reverse flow effects, should be valid up to high rotor advance ratios, if the rotor lift is small, as it must be in this regime for performance reasons. The rotor conditions studied in References (2) and (3) correspond to idling lifting rotors in convertible aircraft, where the rotor is either continuously idling in cruising flight or where low rotor speeds occur during transition in flight to and from a stopped rotor condition. The random flapping response analysis of Reference (2) makes use of the frequency response characteristics of the blades to harmonic inflow variation in the frequency regime of the atmospheric power spectrum. For the planned tests the frequency response characteristics of the blades to harmonic feathering will be determined. This type

of response can also be computed with the help of Reference (4) analysis. Since the blades of the model are very stiff in the chordwise direction, no appreciable pitch-lag-flap coupling effects are expected. The torsional flexibility, though quite high--the torsional blade frequency at normal rotor speed being about 7.5P--may have some effect on the flapping response which could be included with the help of the analysis of Reference (5). Because for the planned test conditions the blade angles of attack will be small and well below stall both for the regions of normal and of reverse flow, and because blade incidence angles and inflow angles will also be small, blade drag can have only a minor effect on the blade flapping response which is mainly determined by lift forces at small lift coefficients. For this reason only the lift slope for normal and reversed flow and its dependence on the input frequencies determines the flapping response. The smallness of the model scale should, therefore, not cause large deviations in blade response as compared to the full scale response. The main question to be answered by the model tests then is, whether or not the concept of quasi-steady aerodynamics in conjunction with the assumption of uniform inflow provides a reasonable approximation for the random blade flapping analysis.

2. The Rotor Model

2.1 Blade

Two sets of blades have been designed and built. Both sets of blades have the following characteristics in common:

(a). Blade radius - 8"

(b). Blade chord - 1"

(c). Blade chordwise C.G. - .25"

Each set has a spring steel .1" by .025" counterweight in its nose. One set of blades is made of redwood and each blade weighs .0145 lbf. One set of blades is made of balsa with a silk and epoxy cover and each blade weighs .0120 lbf. The blade root cross-section is shown in Figure 5. The Lock number of the balsa blade is 4.0 and the Lock number of the redwood blades is 3.4.

A milling tool was formed to produce a NASA 0012 airfoil shape. The milling tool was used to cut the shape out of strips of balsa and redwood. The wood tended to spring back after the milling tool passed over it. Each height element of a cross-sectional area of the airfoil for the two woods was approximately 15% greater than the NASA 0012 airfoil shape called for.

Two formed strips were then glued together - with the counterweight in between - to form the top and bottom of a blade. A 1.5" by .008" by .25" steel shim was also glued into one end of the blade for use in attaching the blade to the hub retention fitting.

The balsa blades were covered with a very fine silk - .002" thick with the fibers running at a 45 degree angle to the leading edge. The silk was painted on with a low viscosity high elastic modulus epoxy (Shell Chemical C. Epon Resin 815 with a TETA amine) creating a very stiff skin on the blade surface. The silk and epoxy added .004" to each height element of the cross-sectional area of the balsa blade or 3% of the maximum thickness. It is intended to ask the Princeton University model shop to provide blades of their own design - fiberglas covered styrofoam - since this shop has considerable experience in building model blades.

Each blade had a calculated first torsional frequency of approximately 300 cps, giving at 40 cps rotor speed a ratio of 7.5P. Phase V-A Report based on Reference (5) gives some indication of the effect of Torsional flexibility on the flapping response to harmonic inflow excitation. Though this effect is not very large, it may have to be considered for an accurate comparison between test results and analysis.

2.2 Blade-Hub Attachment

The blade-hub attachment is stiff in torsion, stiff in the plane of the rotor, and free perpendicular to the plane of the rotor.

The selected design provides for the arms carrying the flapping hinges to be stiff in torsion and soft with respect to axial load and with respect to in-plane moments. Most of

the axial load is carried by the center strap, which also carries most of the in-plane moments.

Figures 3, 4 and 13 show details of the attachment design. The two sets of steel arms carry the load in torsion. The torsional stiffnesses of the arms are 2,700 lbs-in/rad for the set of arms nearest the hub and 250 lbs-in/rad for the set of arms nearest the blade. The blade-hub attachment contributes very little to the flexibility of the blade in torsion.

The edgewise first frequency of the blade is 120 cps. At 40 cps rotor speed this corresponds to a ratio of 3P.

The Oilyte bearing assemblies connecting the arms allow the blades to flap. The friction of these bearings is at present rather high as will be discussed in Section 4.

2.3 Control System

The oscillating shaft, eccentric flexure, and eccentrics are all part of the pitch input control system. Figures 3 and 4 show details of these elements.

The oscillating shaft transmits the pitch input from the eccentric flexure to the blade-hub attachment. The two halves of the oscillating shaft have 12 degrees of rotational freedom so that they can be adjusted with respect to each other and with respect to the eccentric flexure. This permits tracking of the blades.

There are two round Oilyte spacers (Figure 13, not shown in Figure 3 and 4) that extend from either side of the flexure to the hub. They prevent lateral motions of the blade assembly.

The eccentric flexure translates the circular motion of the eccentric into the pitching motion of the oscillating shaft. Three eccentrics with different amounts of eccentricity are available. They have the capability of transmitting ±1.5, ±3.0, or ±4.5 degrees pitching angle to the blade. Each eccentric is fitted with an Oilyte Bearing.

2.4 Drive System

The basic constituents of the drive system are illustrated in Figure 2 and Figure 12. These components are:

1. a rotor drive shaft;
2. a pitch control shaft which rotates the eccentric thus providing a pitch input into the oscillating shaft (Figure 1);
3. a dual motor system driving these two shafts and having a variable speed and reversing capability;
4. a slip ring assembly housing the main support bearings for the rotor drive shaft plus internal bearings for the pitch control shaft;
5. A timing belt drive for the rotor drive shaft and a flexible coupling for direct drive of the pitch control shaft.

The design considerations of the drive system will now be discussed.

First, a high straightness tolerance was necessary due to the long length and the close fit of these shafts. For the pitch control shaft, a .4375 inch drill rod was selected which

easily met the required straightness tolerance. For the rotor shaft, .8125 inch O.D. and .572 inch I.D., no commercial tubing was available with a great enough straightness tolerance to meet the specification of the design. Therefore, oversize tubing was stress relieved and then turned down to the proper size of .8125 inch O.D.

Another consideration was the cantilever frequency of the combined pitch control rotor shaft system which is 103 cps. Since a design maximum speed for the rotor has been set at 50 cps, the operation of the system is confined to less than 50% of the resonant frequency in all cases.

The main support bearings for the rotor drive system are housed in the slip ring assembly which is in turn mounted to a stable support sled to be discussed later. The internal bearings between the pitch control shaft and the rotor drive shaft are oil impregnated bronze sleeve bearings rated at a 70 psi load at the design maximum rpm, a value considerably higher than the anticipated maximum for this application.

The dual motor system was selected because of the necessity of operating both the pitch control shaft and the rotor drive shaft at different rotational speeds to be varied during the test. The motors selected were squirrel cage, A.C. induction motors using an eddy-current clutch to obtain speed regulation. The rotor drive shaft motor is a 1/2 H.P., 50-1600-rpm motor having a full load torque of 35 in-lbs. The shaft is driven through a 2.19 speed ratio sprocket system incorporating

a rubber gearbelt, chosen due to its low slip features and essentially maintenance free operation. This drive system gives a speed range of 110-3500 rpm (2-58 cps) more than the 3000 rpm (50 cps) required for the tests. The motor for the pitch control shaft is of the same type as the rotor drive motor except that the pitch control shaft will be directly driven through a flexible coupling system. The motor is a 1/2 H.P., 65-3300 rpm (1-55 cps) design having 9 in-lbs full load torque and 18 in-lbs starting torque. This drive is reversible so that by operating the dual motor system, the relative rpm between the shafts may be varied from 0-113 cps although 100 cps will be the highest rpm receiving test considerations. Computed torque requirements for both the rotor drive shaft and the pitch control shaft indicate values far below the running torque of either rotor. The slip ring assembly was found to be sensitive to mechanical vibrations coming through the frame and pitch control shaft from the motors. The motors were hand balanced at Washington University, which reduced the eccentricities by a factor of ten, and a number of different couplings were tried between the pitch control motor and the pitch control shaft. The best coupling was found to be a piece of 1"O.D. by 2.5" long Tygon (flexible plastic) piping with a .125" wall thickness mounted on collars on the motor and pitch control shafts. This flexible piping compensated for misalignments much better than commercially available couplings. It also greatly damped out vibrations coming from the motor

shaft to the pitch control shaft.

2.5 Mounting System

The mounting system used consists of two basic parts: (1) the main tunnel support carriage which carries the weight of the tunnel floor, see Figure 1; and (2) the rotor support carriage which supports the rotor and drive assembly, see Figure 2 and 12. The rotor support has the ability to adjust the rotor plane by ±5° from horizontal for final calibration. The rotor support carriage is very rigid and thus has a high natural frequency.

3. Measuring Equipment

The basic measured quantities in this experiment are:

1. blade flapping angle
2. blade azimuth angle
3. pitch input azimuth angle
4. the rotor speed
5. the air velocities within the tunnel test section

Nearly all of these measurements are made electronically (Figure 11). The blade flapping angle is measured by use of a strain gage circuit shown in Figure 6. SR-4 strain gages of the Polymide foil type are anchored to both faces of the cantilever flexure between the hub and the blade. Two Wheatstone measurement bridges were constructed to measure flapping response - one on each blade hub attachment center strap. Each bridge has two active arms, one on each side of the strap.

One bridge was constructed with 350 ohm resistors and the other was constructed with 120 ohm resistors. The other two arms of the bridges are on the rotor shaft above the slip ring assembly. Power to the bridges comes from a Hewlett Packard 7706B Thermal Recording System driver preamplifier power supply which supplied 2400 cycle 5V rms power to the bridge. The bridge outputs are amplified by Hewlett Packard carrier preamplifiers model #8805A.

The power to the bridge and the signal from the bridge have to be translated from a rotating to a stationary frame of reference. This is done through slip rings. The slip rings have silver graphite brushes and coin silver rings having a maximum contact resistance error of .02 ohm. This resistance variation introduces error of less than 1% when the proper circuit is used (Figure 6).

The azimuth angles of the rotor shaft and the pitch control shaft are determined by two magnetic pickups. The pickups convert the mechanical motion of the shafts to A.C. voltage with a frequency proportional to the rpm of the shaft. By simultaneously recording the blips produced by the two rotating shafts, it is possible to determine both the rotative speed of each of the shafts and also the relative position of each shaft at each instant.

The output of the strain gage amplifiers (the carrier preamps) and the magnetic pickups can be monitored in a number of ways depending upon the use that one wants to make of the data.

For initial adjustments the signals can be handily monitored on an oscilloscope. If one is interested in the amplitude and phase characteristics of the signals, a recording oscillograph using light galvonometers which have flat frequency response characteristics from 0-600 cps and light sensitive recording paper is available. If one is interested in the frequency response characteristics of the signal, a 7 track FM tape recorder with 6 speeds is available to record the signals. The tape recorder can be played back through a PDP-12 computer which has an analog to digital converter. The digital information can then be put on cards. This computer has the ability to handle some frequency analysis, but most analysis will be done on the central IBM 360/50 computer. The entire measuring equipment is shown in Figure 13. To the far left is the Ampex FM tape recorder, in left center is the Hewlett Packard Thermal Recording System, of which only the preamplifiers are used, in the right center is the oscilloscope, behind it the oscillograph and the rotor assembly, and to the far right is the control box for the rotor controls.

The tunnel air speed is found by use of a pitot tube in the tunnel test section sufficiently far ahead of the rotor so as not to disturb the flow appreciably.

4. Calibration

The two Wheatstone bridges were calibrated statically by attaching a piano wire to the blade-hub attachment then stringing

the wire over a pulley, and attaching weights to the other end of the wire. In this way centrifugal loads of 1 through 5 kgs were simulated. In order to bend the attachment through an angle, weights were added to the wire between the attachment and the pulley. The deflection of the attachment was measured with a micrometer placed at the end of the blade retention fitting. For each angle measured with the micrometer, a strain gage amplifier output voltage reading was taken. The calibration curves for the two bridges are shown in Figures 7 and 8.

This method of calibration allows one to determine the amount of reading error due to friction in the blade-hub attachment. By carefully loading and unloading the weights onto and off of the wire between the attachment and the pulley, one can determine the reading error due to friction by noting the angular difference between the before and after unloaded positions. A plot of this reading error versus centrifugal load is given in Figure 9. The rotor will be operating in the 5 kg centrifugal load range where the reading error due to friction is on the order of ±.075 degrees. This amounts to a friction moment of 2.5% of the aerodynamic damping moment in hovering for ±2° flapping. There is a good chance that this friction moment will be considerably reduced after the rotor has been run a while and the bearings become seated.

In order to check the calibration constant on the running rotor an optical system to calibrate the blade deflections

dynamically has been designed and built, but not installed. Ray optics can give a precise measure of the deflection of the blades while the rotor is running, so several optical calibration points should be an excellent check on the weights and pulley static calibration. The system is diagrammed in Figure 10. The lense holder angle θ, the photo plate holder angle ϕ, and the distance F are all adjustable. The lense holder will accommodate several different lense sizes. Polished rod mirrors are to be set in the blade 1.4" from the rotor center on the pitching angle input axis. The system is very versatile, i.e., the illuminated area can be expanding by adjusting F, and the combined pitching and flapping motion can be observed directly by placing a plate of ground glass in the photo plate holder.

5. Test Runs

It takes about one-half an hour to track the rotor. The rotor and pitch control shafts are first coupled together so that there is no cyclic pitch input to the blades. The first positioning of the eccentric flexure and the two blade-hub attachments is a guess. The tips of the two blades are painted different colors so that with the rotor turning, one can see how far out of track the blades are running, and at the same time tell which blade is running high and which blade is running low. The blades are then repositioned, by loosening and

retightening the screws in the oscillating shaft, with a set of pointers attached to the blade-hub attachment which point to a degree scale. With successive trials, the blades can be made to run in track to within two-tenths of a degree.

The early runs in hovering beginning in February, 1971 showed varying amounts of noise in the straingauge signals when blade pitch was oscillated. At one per rev. (with only the rotor shaft turning) the signal was almost clean. At higher blade pitch frequencies (greater than 1P) - with the pitch control shaft turning in the opposite direction to the rotor shaft - spikes appeared with an amplitude on the order of magnitude of the amplitude of the signal. The frequency of appearance of the spikes went up as the pitch control motor speed went up, making readings of the signal impossible beyond 1.4 per rev. At lower blade pitch frequency (less than 1P) - with the pitch control shaft turning in the same direction as the rotor shaft - the same spikes appeared except that the frequency of appearance of these spikes went up much faster with pitch control motor speed than in the above 1 per rev case.

The first probable cause of the noise was thought to be an excitation to the blade-hub attachment produced by the pitch control shaft bouncing on the angular and lateral misalignment compensation springs of the Thomas Flexible Coupling then being used between the pitch control shaft and pitch control motor (Figure 2 and 3). Two collars were designed to prevent this possible motion. One collar fits between the

pitch control eccentric and the top Oilyte bronze bearing (Figure 1). The other collar fits on the pitch control shaft and runs against the bottom Oilyte bronze bearing. These collars did not influence the noise.

The next suspected source of the noise was abnormal slip ring resistance variations caused by mechanical vibrations produced by the motors. To verify this assumption, a dummy bridge was built on the rotor shaft. The dummy bridge exhibited the same noise characteristics as the active one, therefore the noise had to be coming from abnormal slip ring resistance variations caused by vibrations of the mechanical system. Since the slip ring assembly provides the main support bearings for the rotor shaft, the first thing done was to greatly stiffen the slip ring assembly. This did not change the noise. Next the mounting frame was greatly stiffened, this also had no effect on the noise. The motors and the slip ring-rotor assembly were then mounted on vibration absorbing pads. This step had no effect on the noise. Next, two things were done in the same step. The motors were balanced (Sec. 2.4), and different pitch control motor to pitch control shaft couplings were tried.

Different couplings were tried, because it was found that if one ran the rotor motor, disconnected the coupling, and retarded the pitch control shaft to varying degrees (corresponding to the less than 1 per rev cyclic pitch excitation case),

one got an almost clean signal. This observation led to the assumption that lateral misalignments between the pitch control motor and pitch control shaft were causing the slip ring brushes and rings to move in opposite directions parallel to their plane of contact. This assumption was the only one which could explain why the frequency characteristics of the noise would be different for the above, and below 1 per rev cases. A flexible plastic pipe coupling was found to be satisfactory (Sec. 2.4, Figure 12).

The noise spikes were totally eliminated and the only noise that remains are some very small amplitude 60 cycle spikes amounting to about a .1 degree signal which may originate from possible electrical discharges in the motors. The stand is well grounded and the circuits well shielded. Should the remaining small amplitude noise interfere with the data analysis, efforts will be made to eliminate it by further shielding or circuit modifications in the motors.

6. Natural Frequencies

All elements of the pitch control system - which includes the vertical pitch control shaft in torsion, the eccentric flexure in bending, the oscillating shaft in torsion, and the arms of the blade-hub attachment in bending - were found to be at least two orders of magnitude stiffer than the torsional blade stiffness. So the first natural frequency of the system

in torsion is essentially that of the blade. The measured stiffnesses of a sample redwood blade and of a sample balsa-epoxy covered blade were both 30 lbf-in^2/rad. Area moments of inertia were found graphically. The first torsional frequency of the redwood blade was calculated to be 310 cps. The first torsional frequency of the balsa blade was found to be 405 cps. A 20 percent error would not be unexpected between the calculated and the real figures. The blades are essentially uncoupled.

The first frequency of the eccentric flexure in torsion (in torsion the flexure carries a .25" dia. by .15" long steel plug that fits into the eccentric) was calculated to be 144 cps. The in-plane first frequency was calculated to be 120 cps. The first frequency in flapping in the non-rotating frame of reference for the blade-hub attachment and blade is 17 cps, or at 40 cps rotor speed, 1.15P.

7. Concluding Remarks

At the end of the first year of development of experimental methods rotor and test equipment are in a working condition, though only qualitative test runs have been made as yet. Several months of delay in the beginning of the tests were caused by the search for the sources of substantial noise in the electrical signals. Though probably of no concern with respect to the blade flapping characteristics, the blades are not as smooth as

desirable and the airfoil shape is somewhat distorted. Otherwise the rotor assembly and testing equipment is working very well and valuable results can be expected in the future. A proposal for extending the development of experimental methods through FY 1972 and 1973 has been submitted.

8. References

1. Gaonkar, G.H. and Hohenemser, K.H., "Flapping Response of Lifting Rotor Blades to Atmospheric Turbulence", Journal of Aircraft, Vol. 6, No. 6, pp. 496-503, Nov.Dec. 1969.

2. Gaonkar, G.H. and Hohenemser, K.H., "Stochastic Properties of Turbulence Excited Rotor Blade Vibrations", AIAA Journal, Vol. 9, No. 3, pp. 419-424, March 1971.

3. Gaonkar, G.H. and Hohenemser, K.H., "Comparison of Two Stochastic Models for Threshold Crossing Studies of Rotor Blade Flapping Vibrations", AIAA Paper No. 71-389 presented at the AIAA/ASME 12th Structures etc. Conference, Anaheim, California, April, 1971.

4. Sissingh, G.J., "Dynamics of Rotors Operating at High Advance Ratios", Journal of the American Helicopter Soc., Vol. 13, No. 3, pp. 56-63, July 1968.

5. Sissingh, G.J. and Kuczynski, W.A., "Investigations on the Effect of Blade Torsion on the Dynamics of the Flapping Motion", Journal of the American Helicopter Soc., Vol. 15, No. 2, April 1970.

Appendix A

List of Borrowed and Purchased Components

Borrowed

1. Rotor Drive Motor
   Eaton-Yale 1/2 H.P., 1600 rpm Adjustospeed Motor, #5041
2. Tektronix Type 502A Dual Beam Oscilloscope
3. AMPEX FR-1300 Recorder/Reproducer
4. Hewlett Packard Thermal Recording System 7706B
5. Consolidated Electrodynamics Corporation Type 5-124 Recording Oscillograph
6. Various Decade Resistance Boxes

Purchased

1. Airelyte Electronic Co. - Type CAY 125 Slip Ring & Brush Block Assembly
2. 3 - C.E.C. Standard Performance Galvanometers, Type 7-323
3. Eaton-Yale - Model #5041 Adjusto-speed Motor, 1/2 H.P., 65-3300 rpm
4. Thomas-Rex Flexible Coupling - Style 50CB
5. Morse Timing Belt Drive System
6. Rapistan - Model 3300 HTO Swivel Casters
7. 2 - Airpax Model 700-0941-A High Sensitivity Magnetic Pickups

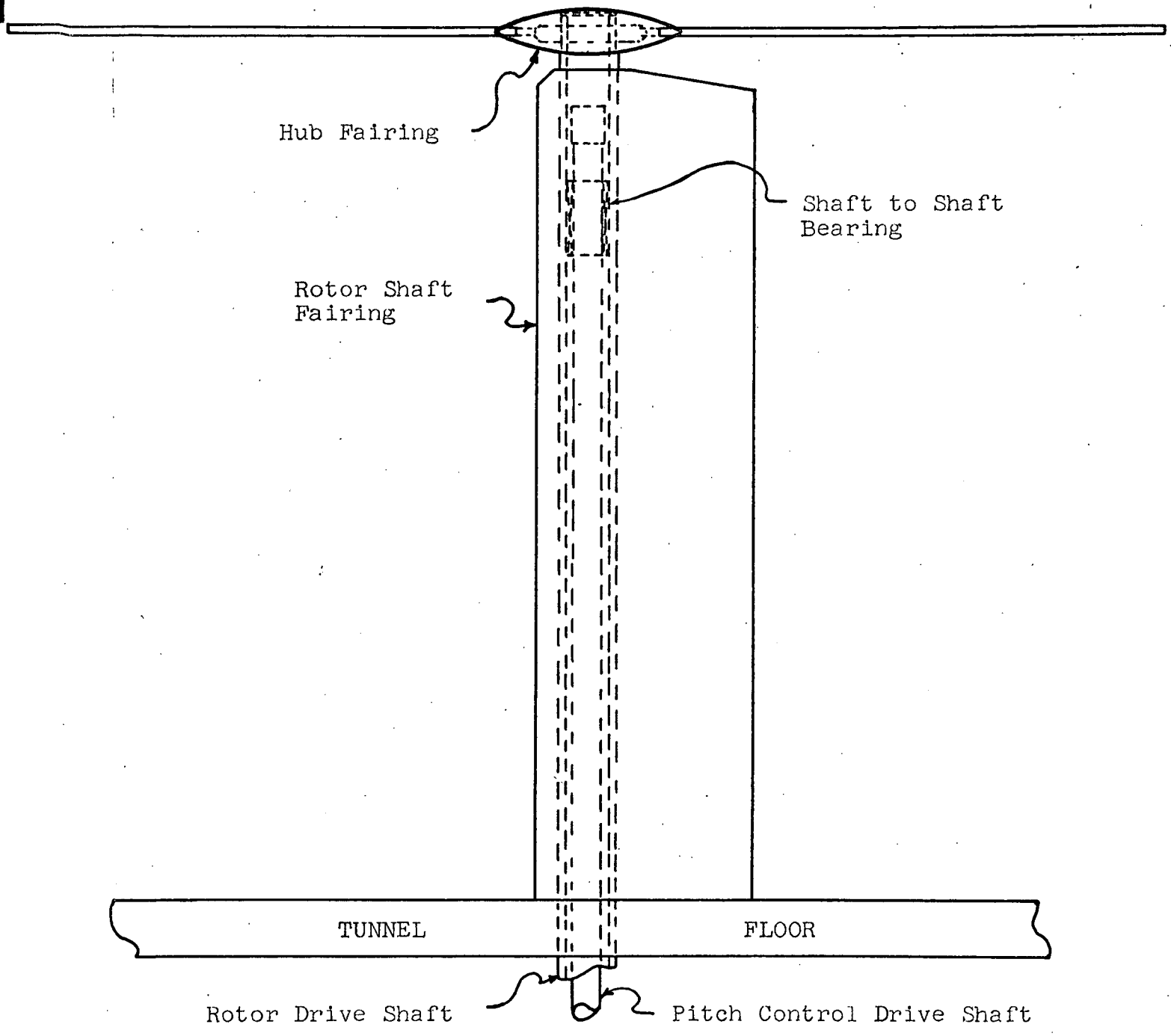

UPPER DRIVE ASSEMBLY

FIG. 1

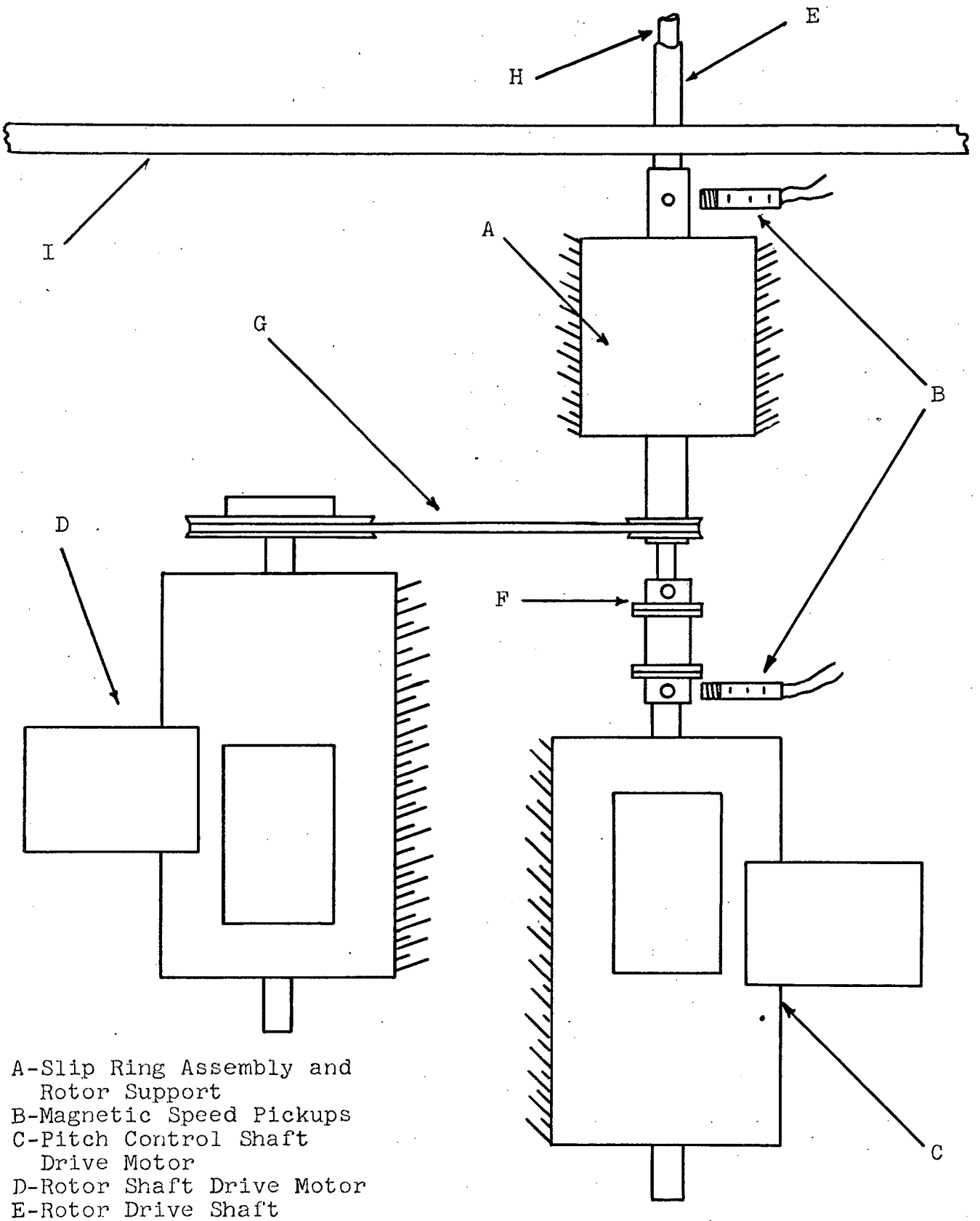

A-Slip Ring Assembly and
  Rotor Support
B-Magnetic Speed Pickups
C-Pitch Control Shaft
  Drive Motor
D-Rotor Shaft Drive Motor
E-Rotor Drive Shaft
F-Flexible Coupling
G-Timing Belt Drive System
H-Pitch Control Shaft
I-Floor of Tunnel Test Section

LOWER DRIVE ASSEMBLY

FIG. 2

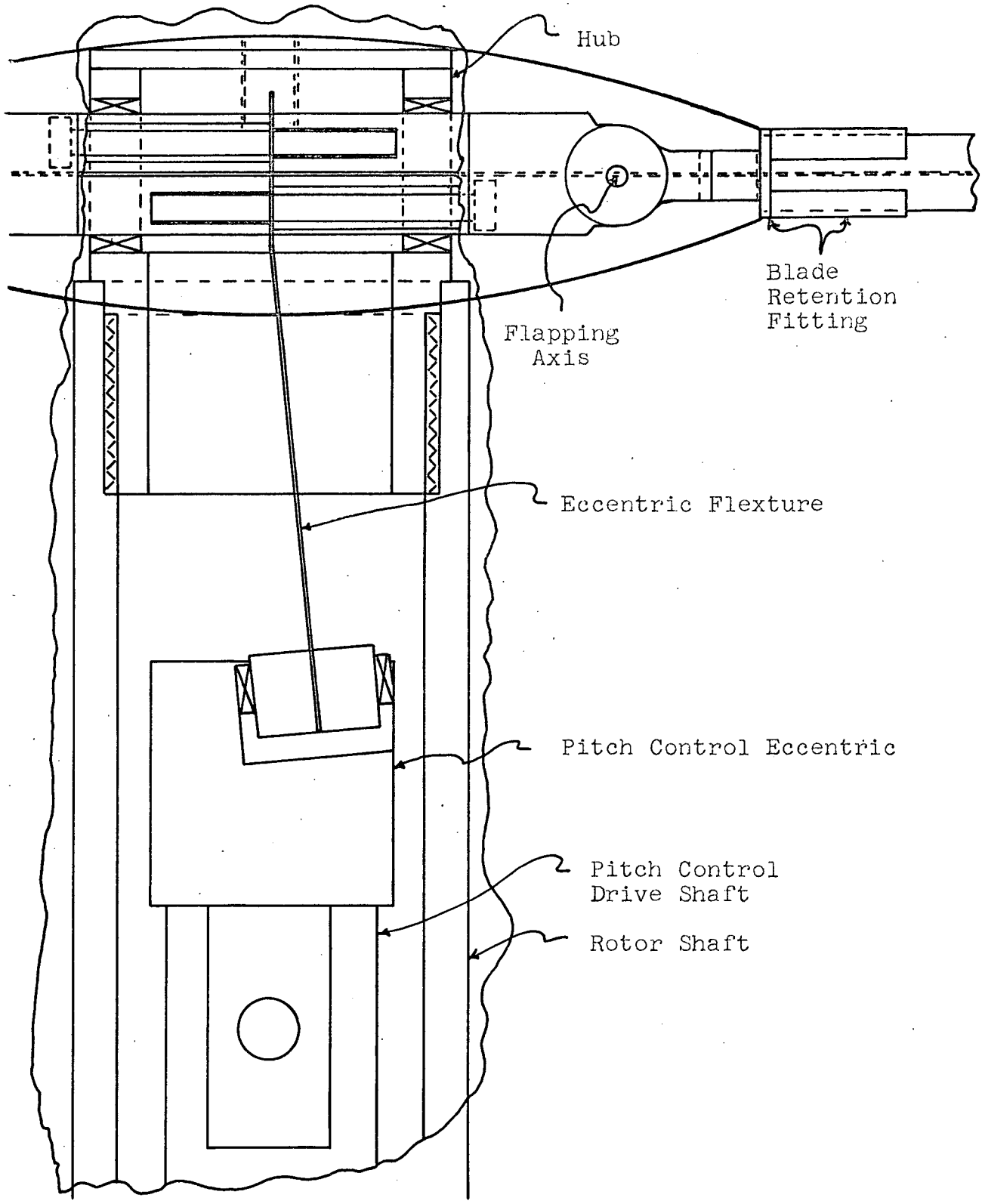

SIDE VIEW: ROTOR AND PITCH CONTROL SYSTEMS

FIG. 3

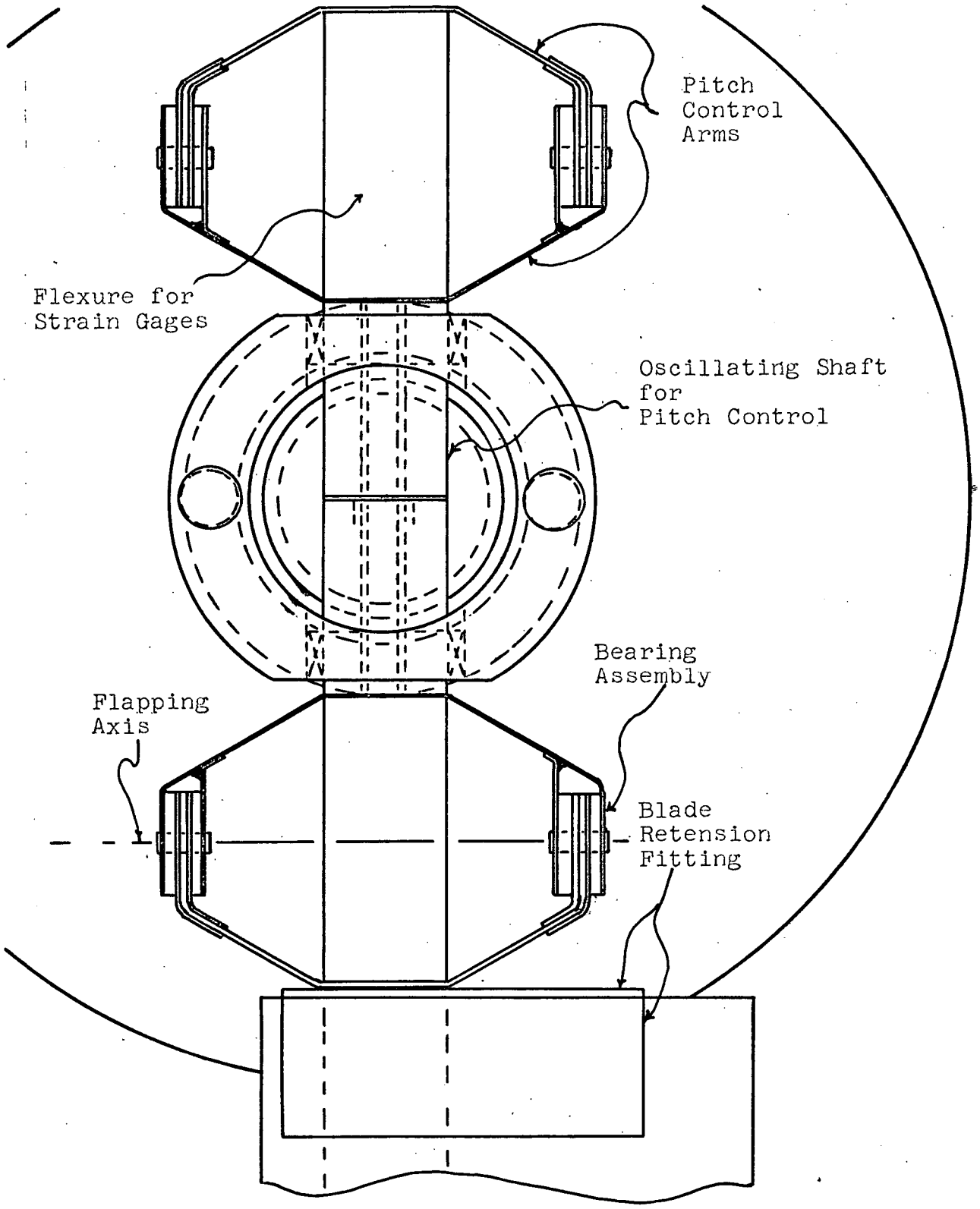

TOP VIEW OF FIG 3

FIG. 4

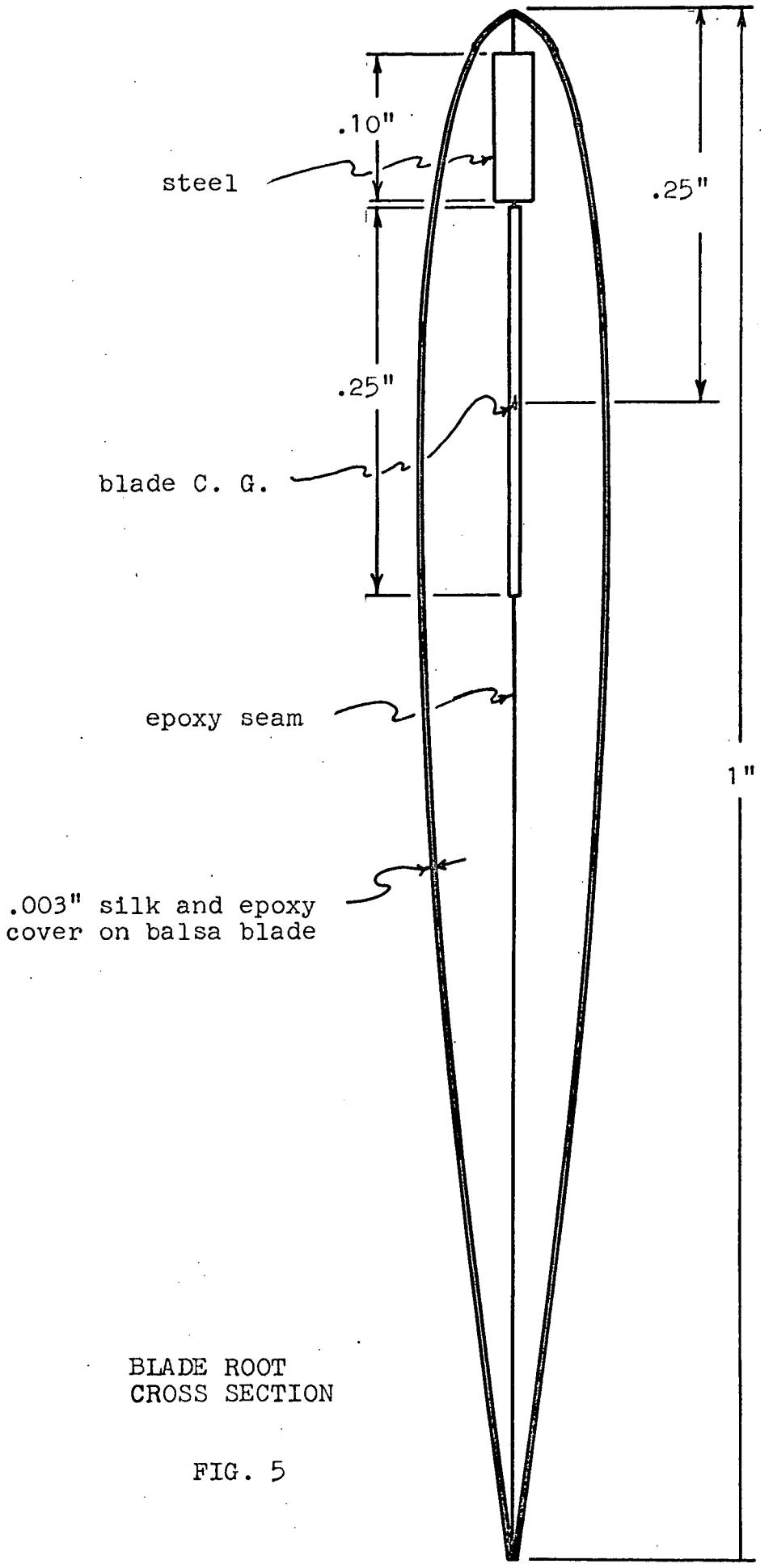

BLADE ROOT
CROSS SECTION

FIG. 5

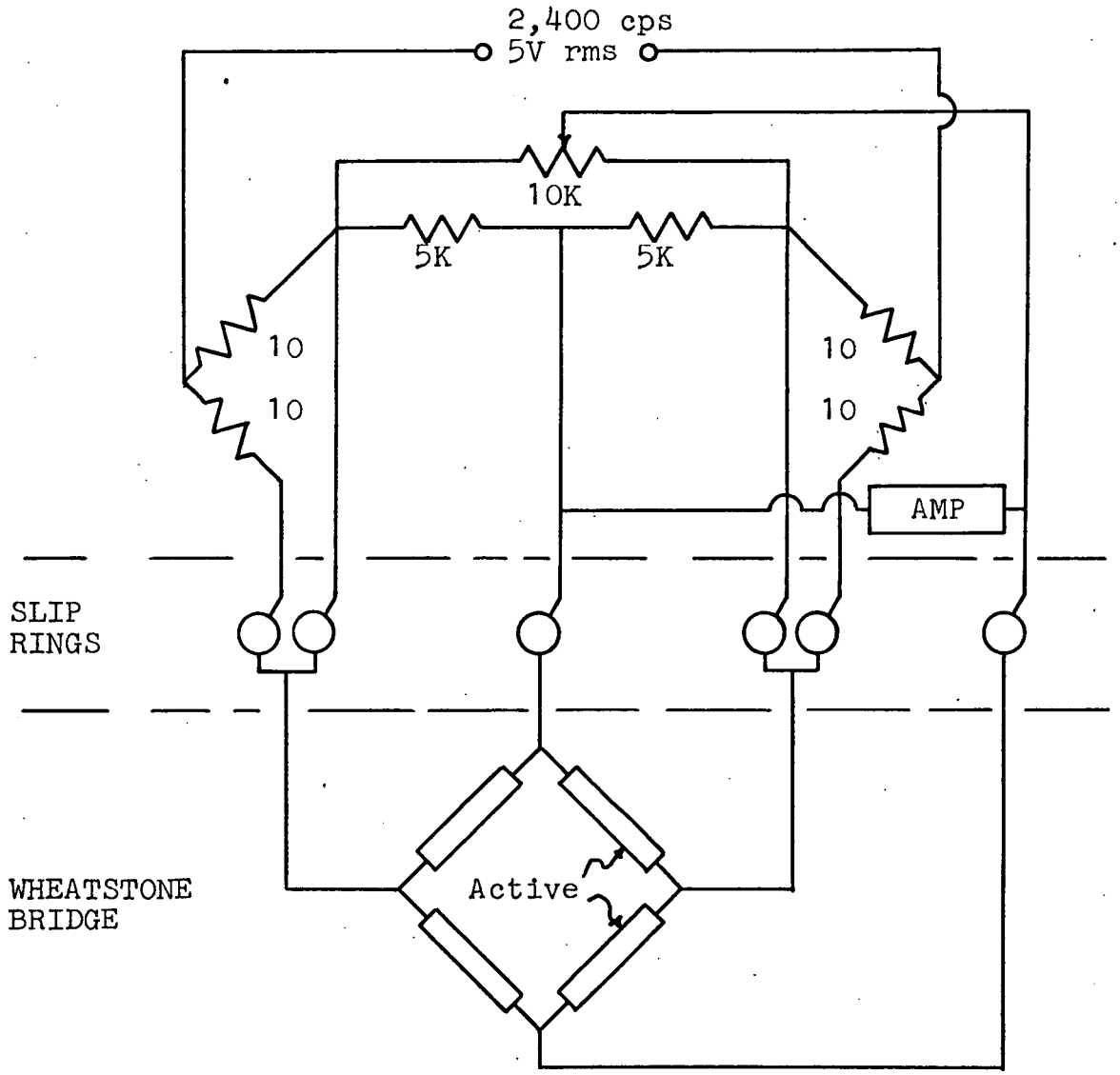

STRAIN GAGE CIRCUIT

FIG. 6

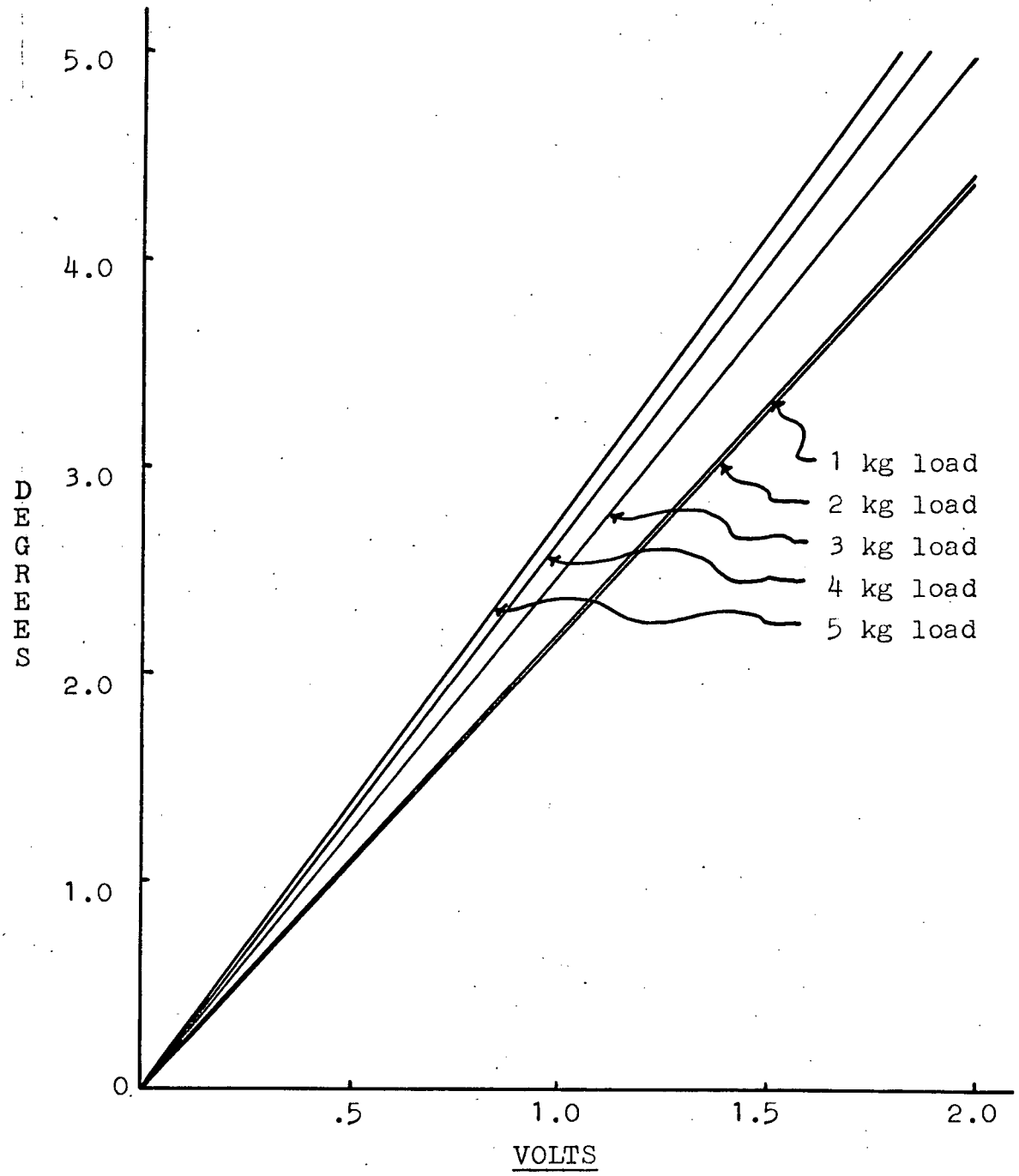

Calibration curve for the 120 ohm bridge using a Sanborn Model 311 strain gage amplifier at 50 X attenuation.

FIG. 7

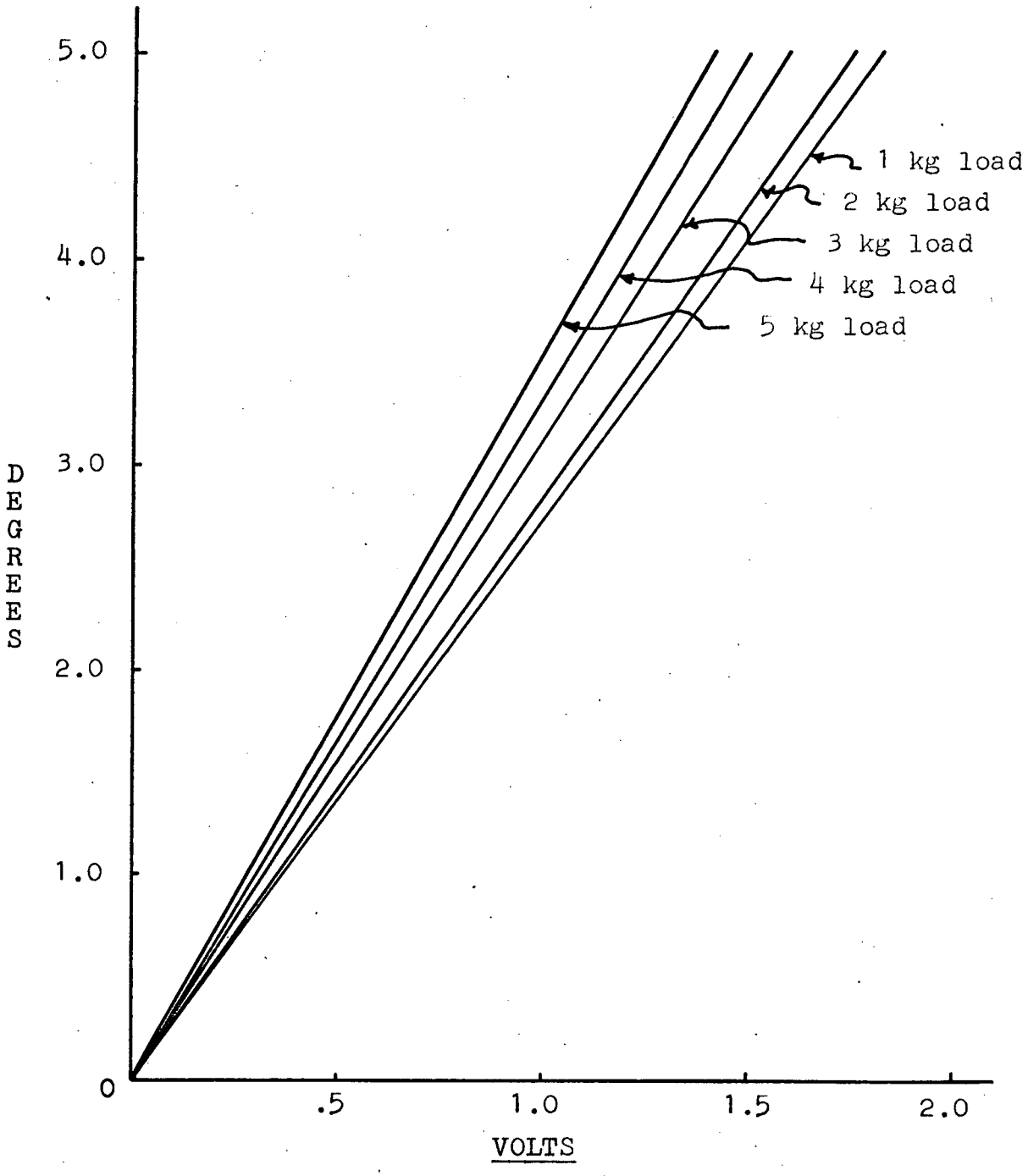

Calibration curve for the 350 ohm bridge using a Sanborn Model 311 strain gage amplifier at 50 X attenuation

FIG. 8

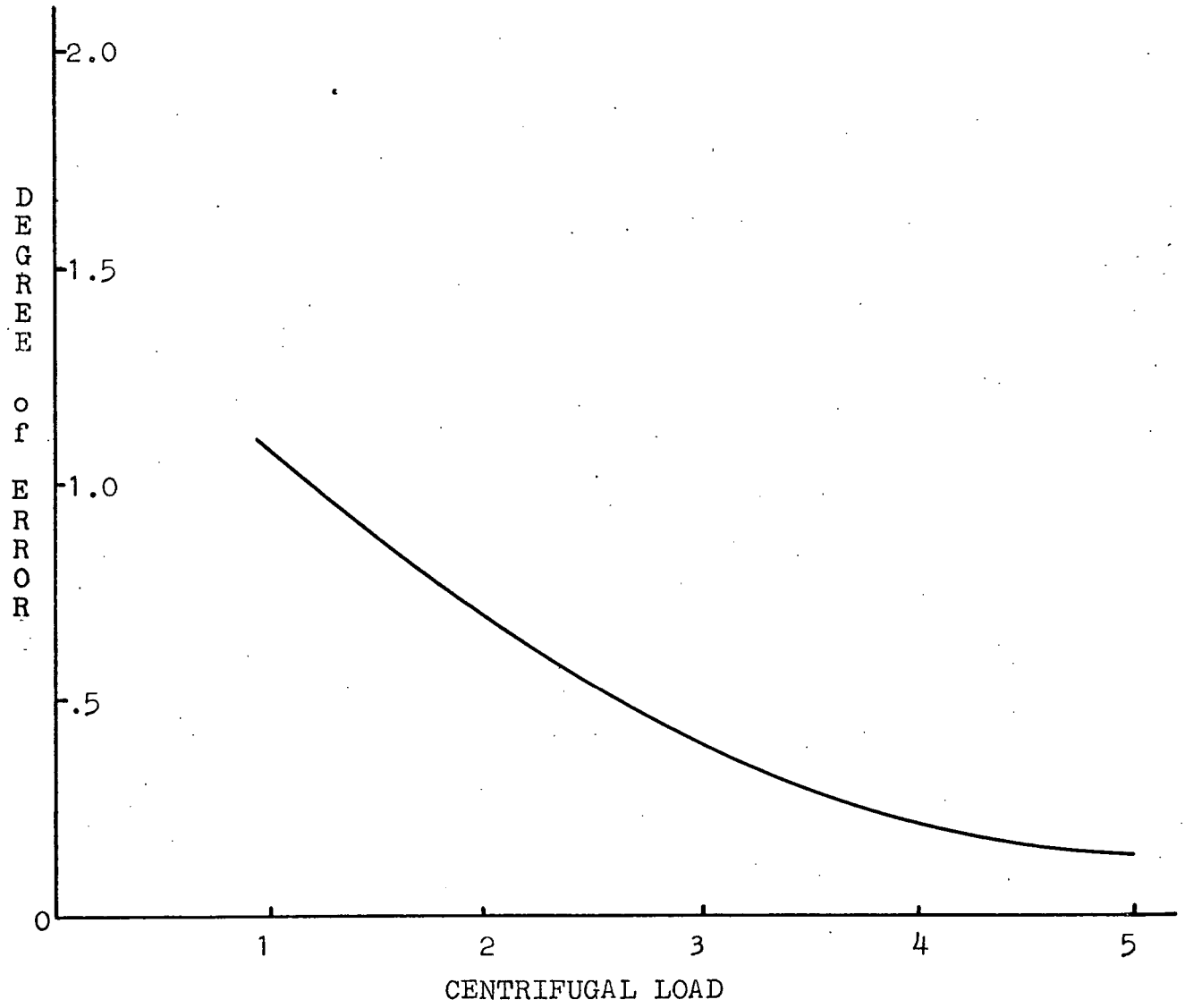

Damping in Blade-Hub Attachment

FIG. 9

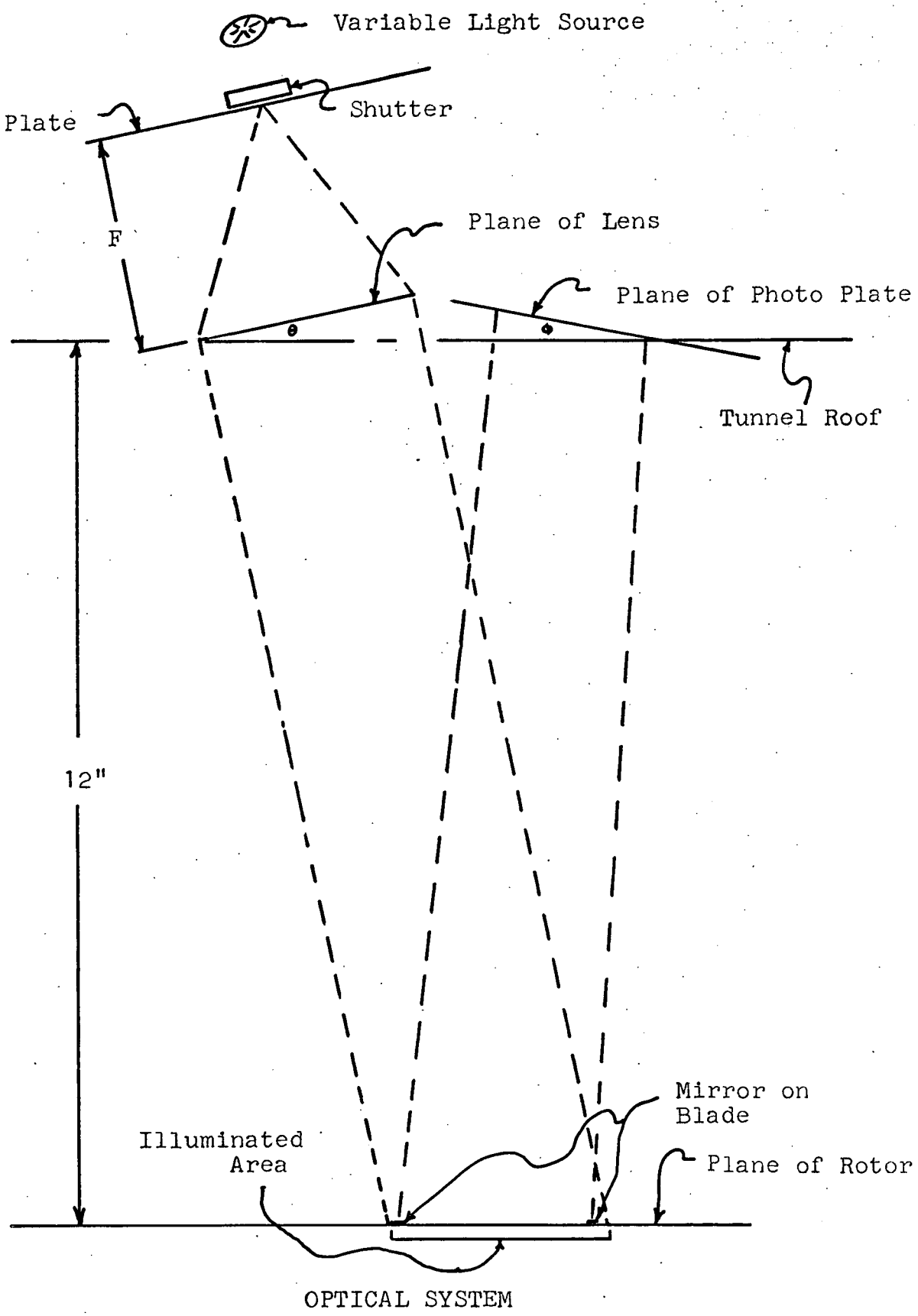
Variable Light Source
Plate
Shutter
F
Plane of Lens
Plane of Photo Plate
θ
Φ
Tunnel Roof
12"
Mirror on
Blade
Illuminated
Area
Plane of Rotor
OPTICAL SYSTEM

FIG. 10

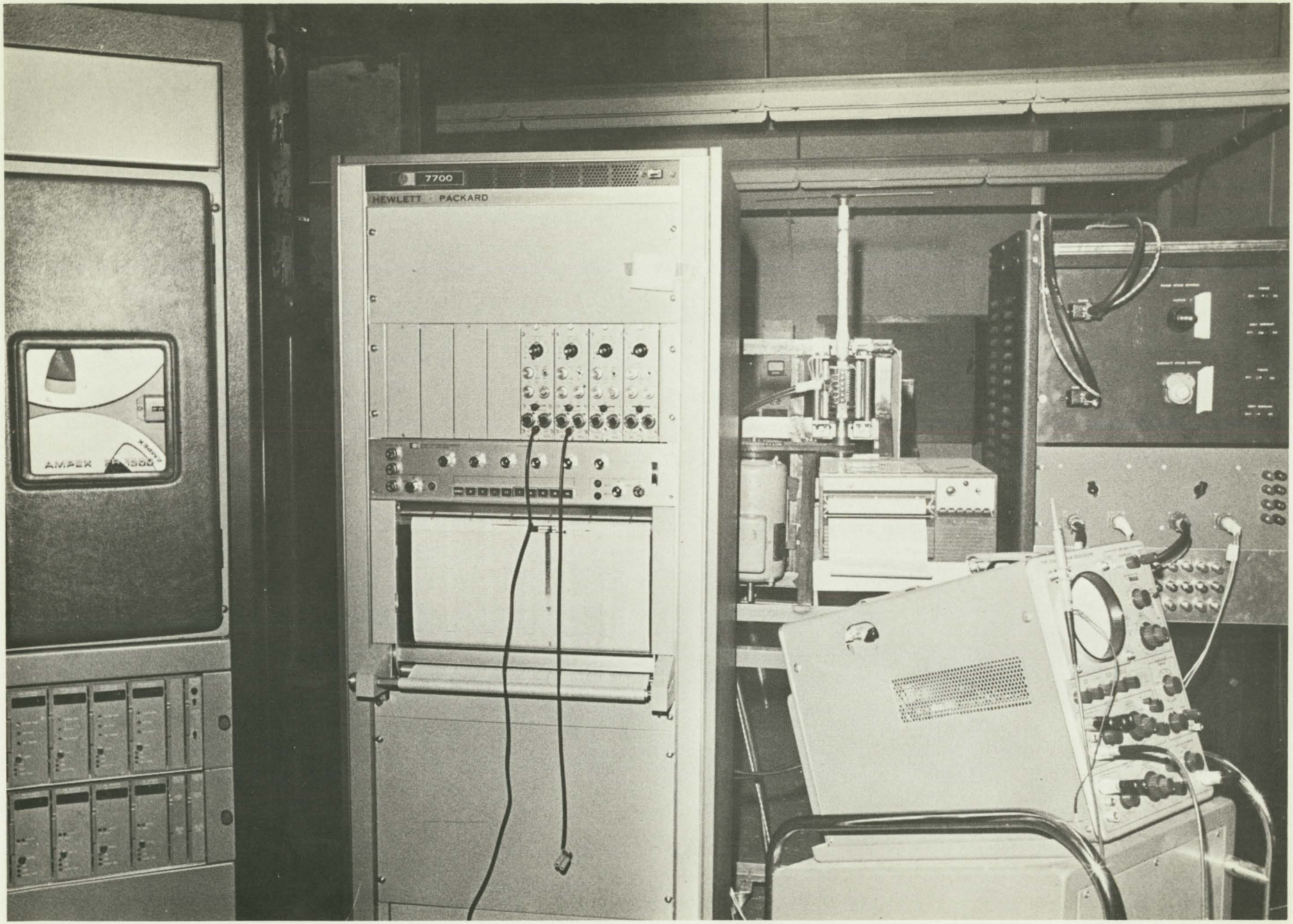

FIGURE II - Control and Recording Equipment

FIGURE 12 - Rotor Assembly

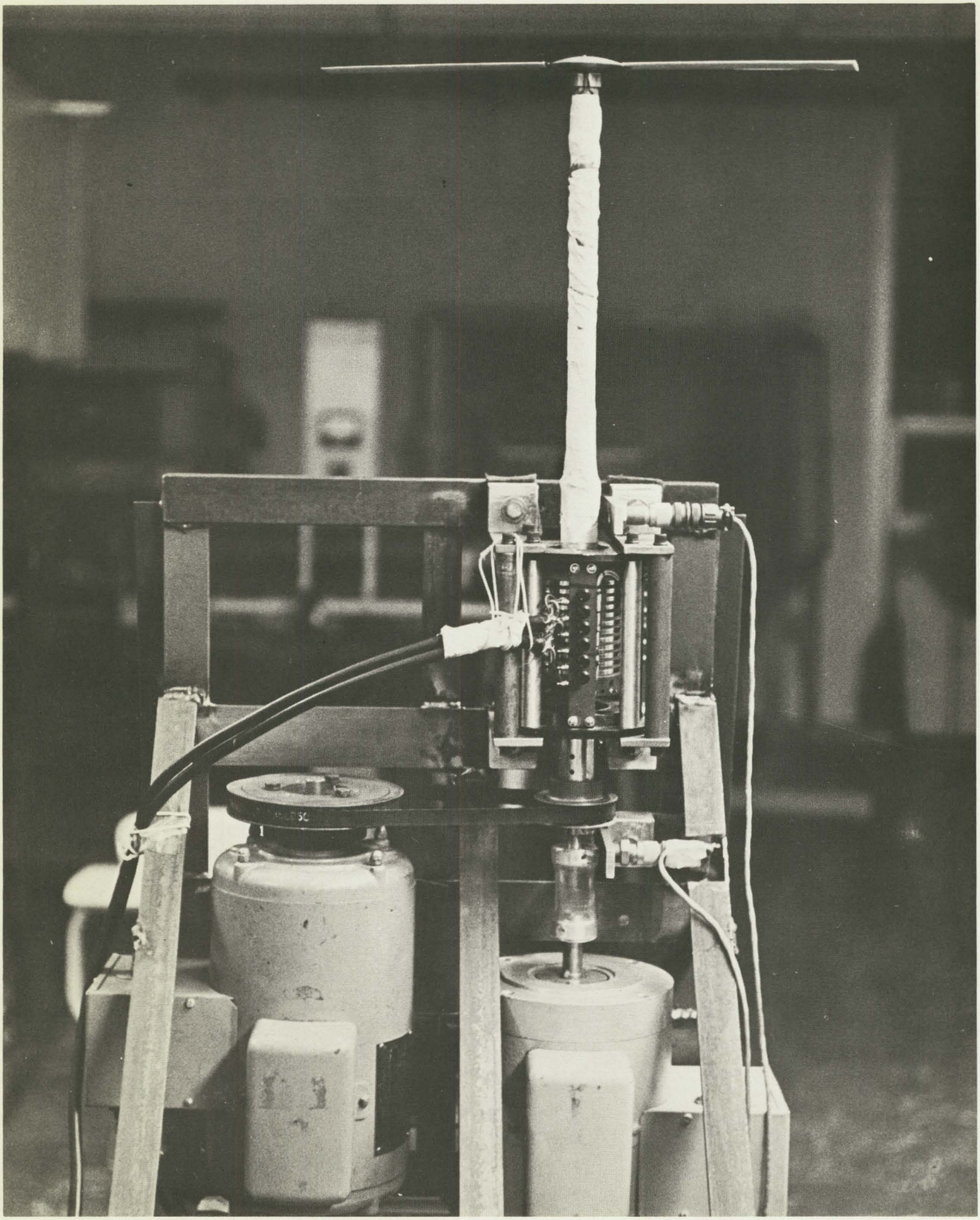

FIGURE 13 - Hub-Blade Attachment